IEEE Access
Multidisciplinary ⋮ Rapid Review ⋮ Open Access Journal

Received 6 October 2024, accepted 5 November 2024, date of publication 12 November 2024, date of current version 22 November 2024.

Digital Object Identifier 10.1109/ACCESS.2024.3496790

RESEARCH ARTICLE

Influence of Parameter Variation in Analytical Preisach Model on Shape of Hysteresis Loop

HUIYING ZHANG[1,2], YADONG SHEN[2], AND MINGXING TIAN[1,2]

[1]School of Automation and Electrical Engineering, Lanzhou Jiaotong University, Lanzhou 730070, China
[2]Rail Transit Electrical Automation Engineering Laboratory of Gansu Province, Lanzhou Jiaotong University, Lanzhou 730070, China

Corresponding author: Huiying Zhang (zhanghylz@163.com)

This work was supported in part by the Natural Science Fund of Gansu Province under Grant 24JRRA244, in part by the National Natural Science Fund of China under Grant 52167013, and in part by the Key Project Natural Science of Gansu Province under Grant 22JR5RA320.

ABSTRACT The Analytical Preisach Model (APM) describes the magnetization characteristics of materials with high accuracy and good universality, and the corresponding mathematical equations of the model are analytical expressions, which makes it very easy to solve and calculate. The distribution function parameters of APM are the main influencing factors on the shape of the hysteresis loop. In this paper, coercive force, remanence point, vertex magnetic induction intensity, area, rectangular ratio, and inclination of the hysteresis loop are used as comparative indicators for the shape of the hysteresis loop. The sensitivity analysis of the influence of distribution function parameter value changes on the hysteresis loop shape is conducted using the single factor variable method. The parameter values vary within the range of 0.9-1.1 times the baseline value, and when one parameter changes, the other parameters remain unchanged. By observing and analyzing the shape of the hysteresis loop before and after parameter changes and comparing the numerical values of the indicators, the law of the shape of the hysteresis loop changing with parameters can be obtained. The results show that some parameters have a low sensitivity to changes in the hysteresis loop shape, while others have a high sensitivity and cause significant variations. Furthermore, the direction of change in the shape indicator varies depending on the parameter. Some indicators increase with parameter increase, while others decrease. This information can be used to guide the correction of APM parameter values.

INDEX TERMS Magnetization characteristic, analytical Preisach model, magnetic hysteresis loop, parametric effect analysis.

I. INTRODUCTION

The Preisach hysteresis model is suitable for simulating the magnetization characteristics of various magnetic materials and is widely used for modeling the magnetization characteristics of electromagnetic equipment or power electronic devices containing magnetic cores [1], [2], [3]. The Classic Preisach Model (CPM) has high accuracy in simulating the magnetization characteristics of materials [4]. Still, its solution process requires storing the distribution function in advance, resulting in a longer computation time [5], [6]. The comparison of the calculation times of CPM, Jiles-Atherton (J-A), and D'Aloia-Di Francesco-De Santis (D-D-D) models in reference [7] also confirms this issue. Although the CPM calculation time is significantly shorter than that of the J-A model, it is longer than that of the D-D-D model. To solve the problem of long computation time in CPM, reference [8] introduced a special analytical function to transform the distribution function of CPM into an analytical function, resulting in the Analytical Preisach Model (APM). Reference [9] corrected the errors in the distribution function expression in reference [8] and obtained a correct and universal APM. While solving the APM, there is no storage requirement for its distribution function, resulting in higher computational efficiency. To achieve the goal of reducing computation time, some scholars have used known functions to approximate the distribution function of CPM and obtain a simplified distribution

The associate editor coordinating the review of this manuscript and approving it for publication was Valerio De Santis.

function [10], but approximate substitution may bring errors.

At present, research on the APM mainly focuses on two aspects: model extension and parameter identification. In [11] and [12], an extended model was obtained by introducing the effect of temperature on the magnetization characteristic. References [13] and [14] considered reversible magnetization components and obtained an extended model of the APM accounting for both reversible and irreversible magnetization components. Aiming at the problem that the model parameters of APM are many and complicated to identify, many scholars have proposed to use optimization algorithms to determine the values of model parameters, such as the chimpanzee algorithm [15], particle swarm algorithm [12], differential Evolution Algorithm [16], and non-uniform element discretization method [17] and so on. In addition, some scholars have proposed non-uniform segmentation methods to reduce the number of segments in Preisach triangles and improve solving speed [18]. Currently, there is a lack of research, both domestically and internationally, on the effects of APM parameters on the hysteresis loop. The magnetization processes includes the irreversible magnetization process and the reversible magnetization process, with irreversible magnetization process dominating [19], [20]. The APM parameters can be divided into irreversible magnetization component characteristic parameters and reversible magnetization component characteristic parameters.

The distribution function parameters of APM are characteristic parameters that describe irreversible magnetization components and are also the main factors affecting the shape of hysteresis loops. Therefore, this article mainly studies the influence of the characteristic parameters of the irreversible magnetization component of APM on the shape of the hysteresis loop.

Therefore, to address the problem of unclear laws regarding the effect of parameter changes in the APM on the hysteresis loop, this paper adopts a univariate control method to analyze the influence of the irreversible magnetization component characteristic parameters of APM on the shape of the hysteresis loop. Through quantitative analysis, the trend and pattern of hysteresis loop shape changing with parameters are revealed. In some cases, although the initial values of parameters determined by parameter identification can simulate the approximate hysteresis loop, there is still a certain degree of error compared with experimental data. Therefore, it is hoped that the research results of this article will play a role in correcting the parameter values of APM.

II. ANALYTICAL PREISACH MODEL AND SHAPE PARAMETERS OF HYSTERESIS LOOP

There have been three major revisions in the evolution from CPM to APM. First, the Everett integral function was introduced to reduce the storage requirements of the distribution function in the CPM solution process. Secondly, a special analytical function was introduced to obtain the analytical Everett function, which solved the problem of pre-storage in the solution process and obtained the APM based on the analytical Everett function. Then, the reversible magnetization component during the magnetization process was added to the APM based on the analytical Everett function, resulting in the APM considering both reversible and irreversible magnetization components. This model is the APM investigated in this paper.

A. PREISACH MODEL BASED ON EVERETT FUNCTION

The CPM is the earliest proposed macroscopic hysteresis model based on the assumption of the hysteresis operator. The Preisach theory assumes that the magnetization properties of magnetic materials consist of many bistable hysteresis units, and that the macroscopic expression of their hysteresis properties consists of the linear superposition of hysteresis basic units. The input of the CPM is the magnetic field strength H, and the output is the magnetic flux density B, and the expression of the CPM is shown in (1) [1].

$$B(t) = \iint_S \mu(h_1, h_2)\gamma[h_1, h_2, H(t)]\mathrm{d}h_1\mathrm{d}h_2 \tag{1}$$

where $\mu(h_1, h_2)$ is the distribution function of the basic unit of magnetization, $\gamma[h_1, h_2, H(t)]$ is the basic unit of magnetization, and the state quantities of each unit of magnetization are only two state quantities, "+1" and "−1", h_1 and h_2 are the positive and negative flipping thresholds of the magnetization basic unit, respectively, and S is the range of values of the Preisach distribution function. The magnetization characteristics of the magnetization unit and the Preisach distribution function are shown in Figure 1.

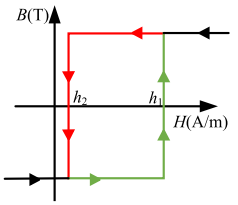

(a) Basic unit of magnetization

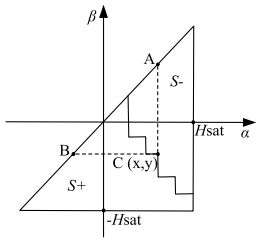

(b) Domain of Preisach distribution function

FIGURE 1. Basic magnetization unit and domain of Preisach distribution function.

To solve the CPM, the distribution function has to be stored on the whole preisach plane, and some scholars have introduced the Everett integral function which effectively

reduces the storage requirement in the solution process and the computational cost. Reference [8] optimized the CPM by introducing the Everett function as shown in (2). The Preisach model is obtained on the basis of the Everett function as in (3).

$$E(x,y) = \iint_T \mu(h_1,h_2)\mathrm{d}h_1\mathrm{d}h_2 = \int_y^x \int_{h_2}^x \mu(h_1,h_2)\mathrm{d}h_1\mathrm{d}h_2 = \int_x^y \int_{h_1}^y \mu(h_1,h_2)\mathrm{d}h_2\mathrm{d}h_1 \tag{2}$$

where the integration domain T is the right triangle ABC in the distribution diagram in Figure1(b), and the current working point C(x, y) is the right angle vertex.

$$B(t)\begin{cases} E[H(t),-H(t)], & H_m = 0, B_m = 0 \\ B_m - 2E[H_m, H(t)], & H \le H_m \\ -B_m + 2E[H(t), H_m], & H \ge -H_m \end{cases} \tag{3}$$

where H_m is the maximum magnetic field strength and B_m is the maximum magnetic flux density.

B. PREISACH MODEL BASED ON ANALYTIC EVERETT FUNCTION

Although the Preisach model based on the Everett function dramatically reduces the storage requirement, it still requires the Preisach graph distribution function to be stored in advance. To address the problem of the pre-storage requirement, some scholars [8] obtain the analytic Everett function and then the analytic Preisach function by introducing a special analytic function. The expression of the analytic Everett function is presented as follows:

$$E(x,y) = \sum_{i=1}^{n} \frac{\alpha^2}{\beta^2} \cdot \frac{e^{\beta_i y} - e^{\beta_i x} + \frac{(\gamma_i + e^{\beta_i x})(1+\gamma_i e^{\beta_i y})}{1-\gamma_i^2} \cdot \ln \frac{(1+\gamma_i e^{\beta_i y})(\gamma_i + e^{\beta_i x})}{(1+\gamma_i e^{\beta_i x})(\gamma_i + e^{\beta_i y})}_i}{(1-\gamma_i^2)(\gamma_i + e^x)(1+\gamma_i e^{\beta_i y})} \tag{4}$$

in (4),

$$\begin{cases} \beta_i = 1/c_i \\ \gamma_i = \mathrm{e}^{b_i/c_i} \\ \alpha_i = a_i \mathrm{e}^{b_i/c_i} \end{cases} \tag{5}$$

where a_i, b_i and c_i are parameters of the distribution function and also characteristic parameters of irreversible magnetization components. The introduction of the Everett function enables the CPM based on the Everett function to be solved analytically and makes the model more convenient to use.

C. ANALYTICAL PREISACH MODEL

The reversible magnetization component is not considered in the Preisach model based on analytic everett function, and the slope at the hysteresis loop slewing point is 0. References [8], [9], and [21] adds the reversible magnetization component to the slewing process of the model, and obtains the APM which includes the reversible magnetization component, and its expression is

$$B(t)\begin{cases} E[H(t),-H(t)] + Brev, & H_m = 0, B_m = 0 \\ B_m - 2E[H_m, H(t)] + Brev, & H \le H_m \\ -B_m + 2E[H(t), H_m] + Brev, & H \ge -H_m \end{cases} \tag{6}$$

in (6),

$$Brev = d_1 H(t) + d_2 \tanh(\frac{H(t)}{d_3}) \tag{7}$$

where d_1, d_2 and d_3 are the coefficients to be determined.

By substituting (4) and (5) into (6), the APM expression that takes into account the reversible magnetization component can be obtained as (8), as shown at the bottom of the next page, where L_1, L_2, L_3, are

$$\begin{cases} L_1 = \ln \dfrac{(1+\mathrm{e}^{b_i/c_i}e^{-H(t)/c_i})(\mathrm{e}^{b_i/c_i} + e^{H(t)/c_i})}{(1+\mathrm{e}^{b_i/c_i}e^{H(t)/c_i})(\mathrm{e}^{b_i/c_i} + e^{-H(t)/c_i})} \\ L_2 = \ln \dfrac{(1+\mathrm{e}^{b_i/c_i}e^{H(t)/c_i})(\mathrm{e}^{b_i/c_i} + e^{H_m/c_i})}{(1+e^{H_m/c_i})(\mathrm{e}^{b_i/c_i} + e^{H(t)/c_i})} \\ L_3 = \ln \dfrac{(1+\mathrm{e}^{b_i/c_i}e^{H_m/c_i})(\mathrm{e}^{b_i/c_i} + e^{H(t)/c_i})}{(1+e^{H(t)/c_i})(\mathrm{e}^{b_i/c_i} + e^{H_m/c_i})} \end{cases} \tag{9}$$

The APM shown in (8) is the object of study in this paper, and its parameters a_i, b_i and c_i are used to control the irreversible magnetization part of the hysteresis loop, and the parameters d_1, d_2 and d_3 are used to control the reversible magnetization part of the hysteresis loop. The irreversible magnetization parameters a_i, b_i and c_i are not a fixed number of parameters, and the number of parameters varies with the value of n. The APM employed in this study provides a computational simulation of the static hysteresis loop. The shape and area of the static hysteresis loop are predominantly determined by the irreversible magnetization component, while the influence of the reversible magnetization component is relatively small. Consequently, this investigation primarily focuses on the influence of the irreversible magnetization parameter on the hysteresis loop.

D. SHAPE PARAMETERS OF HYSTERESIS LOOP

To investigate the influence of irreversible magnetization parameters of APM on the hysteresis loop shape, the paper uses coercivity H_c(unit A/m), remanence point B_r(unit T), magnetic induction intensity at the vertex of loop B_p (unit T), loop area S_hb (unit T•A/m), slope factor $K_\mathrm{cr} = H_\mathrm{c}/B_\mathrm{r}$, and rectangular ratio $K_\mathrm{pr} = B_\mathrm{p}/B_\mathrm{r}$ as shape parameters, which are marked in Figure 2.

In Figure 2, H_c characterizes the width of the hysteresis loop; B_p characterizes the height of the hysteresis loop; use the change of B_r to characterize the change in the inflection point of the loop, and an increase in B_r indicates an increase in the height of the inflection point of the loop; the change in K_cr represents the degree of rightward slope of the loop, and an increase in K_cr indicates an increase in the degree of rightward slope of the loop; S_hb can describe the overall variation of the hysteresis loop; K_pr represents

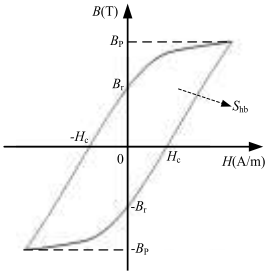

FIGURE 2. Schematic diagram of hysteresis loop shape parameters.

the degree of rectangular hysteresis loop. In this paper, the single factor variable method is used to compare and analyze the changes in H_c, B_r, B_p, S_{hb}, K_{cr} and K_{pr} when the reversible magnetization parameters a_i, b_i and c_i are changed respectively. By quantitatively analyzing the above shape indicators, the effect of parameter changes on the hysteresis loop is demonstrated from different perspectives.

From Figure 2, it can be seen that on the hysteresis loop, when $H = 0$, $B = B_r$. Substituting the point $(0, B_r)$ into (8) gives the calculation expression for B_r, which includes parameters a_i, b_i, and c_i and is a complex function composed of several exponential polynomials. Even under the condition of a single parameter change and constant values of other parameters, it is very difficult to determine theoretically the relationship between B_r and parameter changes from its expression. Similarly, in the case where the magnetic field strength at the loop vertex is H_p = constant, although the expression for B_p can be from (8), it is difficult to determine the relationship between B_p and parameter changes directly from the B_P expression.

On the lower branch of the hysteresis loop, when $H = H_c$, $B = 0$. Substituting the point $(H_c, 0)$ into (8) gives an equation containing H_c, which includes the parameters a_i, b_i, and c_i. H_c appears in the exponent of the equation and is distributed over several polynomials. It is not possible to obtain an expression for H_c represented by the parameters a_i, b_i, and c_i. Therefore, the tendency of H_c to vary with the parameters cannot be obtained directly from the formulas.

The calculation expression for the hysteresis loop area is $S_{hb} = \int BdH$. Due to the complexity of the B expression in (8), it is difficult to convert the integral expression of S_{hb} into an analytical expression, making it impossible to predict the relationship between S_{hb} and parameter changes based on the expression. Therefore, in this article, the parameter values of the APM are changed using an example of a magnetically conductive material to investigate the influence of model parameter changes on the shape of the hysteresis loop.

III. INFLUENCE OF PARAMETER VARIATION IN APM

A. MODEL PARAMETER VALUES

From (8), it can be seen that the APM consists of polynomial functions, the larger the value of n is, the higher the computational accuracy of the model is, but when n is increased to a certain degree, the increase in accuracy is relatively limited. Considering the computational cost and accuracy, it is more appropriate to take $n = 3$ [8], and in this paper, the value of n is taken as 3 during the analysis of the influence of parameter changes. Due to the fact that there are many parameters to be determined in the APM, in order to identify the influence of specific parameters on the hysteresis loop while avoiding the influence of other parameters, this paper uses the one-factor-variable method to investigate the influence of the irreversible magnetization parameter on of the APM on the hysteresis loop.

Reference [9] obtained the parameter values of the APM through parameter identification, as shown in Table 1, including the irreversible magnetization parameters a_i, b_i, c_i and reversible magnetization parameter d_i, and the reliability of the model parameters is verified by comparing the hysteresis loop calculated by simulation and measured ones. In this paper, the values of the irreversible magnetization parameters in Table 1 are taken as the base values, and the magnitude of the parameter values is changed to analyze the effect of parameter changes on the hysteresis loop. Since the effect of the reversible magnetization parameter d_i is not taken into account, the parameter values d_i in Table 1 are kept constant.

TABLE 1. Parameters of APM for a sample of silicon steel [21].

i	a_i	b_i	c_i	d_i
1	0.113	56.468	6.035	9.512×10^{-5}
2	2.224×10^{-3}	10.197	284.54	0.214
3	1.812×10^{-3}	86.148	38.842	362.86

$$B(t) = \begin{cases} \sum_{i=1}^{n} (a_i c_i e^{b_i/c_i})^2 \cdot \dfrac{e^{-H(t)/c_i} - e^{H(t)/c_i} + \frac{(e^{b_i/c_i}+e^{H(t)/c_i})(1+e^{b_i/c_i}e^{-H(t)/c_i})}{1-e^{2b_i/c_i}} \cdot L_1}{(1-e^{2b_i/c_i})(e^{b_i/c_i}+e^{H(t)/c_i})(1+e^{b_i/c_i}e^{-H(t)/c_i})} + Brev, & H_m = 0, B_m = 0 \\ B_m - 2\sum_{i=1}^{n} (a_i c_i e^{b_i/c_i})^2 \cdot \dfrac{e^{H(t)/c_i} - e^{H_m/c_i} + \frac{(e^{b_i/c_i}+e^{H_m/c_i})(1+e^{b_i/c_i}e^{-H(t)/c_i})}{1-e^{2b_i/c_i}} \cdot L_2}{(1-e^{2b_i/c_i})(e^{b_i/c_i}+e^{H_m/c_i})(1+e^{b_i/c_i}e^{H(t)/c_i})} + Brev, & H \le H_m \\ -B_m + 2\sum_{i=1}^{n} (a_i c_i e^{b_i/c_i})^2 \cdot \dfrac{e^{H_m/c_i} - e^{H(t)/c_i} + \frac{(e^{b_i/c_i}+e^{H(t)/c_i})(1+e^{b_i/c_i}e^{H_m/c_i})}{1-e^{2b_i/c_i}} \cdot L_3}{(1-e^{2b_i/c_i})(e^{b_i/c_i}+e^{H(t)/c_i})(1+e^{b_i/c_i}e^{H_m/c_i})} + Brev, & H \ge -H_m \end{cases} \quad (8)$$

B. EFFECT OF PARAMETER a_i VARIATION ON HYSTERESIS LOOP SHAPE

In order to analyze the effect of parameter a_i variation, while keeping the values of b_i, c_i and d_i in Table 1 unchanged, this paper takes the values of a_i in Table 1 as the reference values and multiplies the values of $a_1 \sim a_3$ by the same multiple to achieve an increase or decrease in a_i. The values of $a_1 \sim a_3$ in Table 1 are represented by a_{i0} and multiplied by 0.90, 0.95, 1.05, 1.10 times to obtain four groups of parameter values of a_i respectively. Substituting the four sets of different parameter values into the APM shown in (8). The hysteresis loops corresponding to the different a_i parameter values are obtained by programming as shown in Figure 3, and the values of H_c, B_r, B_p, K_{cr}, S_{hb} and K_{pr} are listed in Table 2.

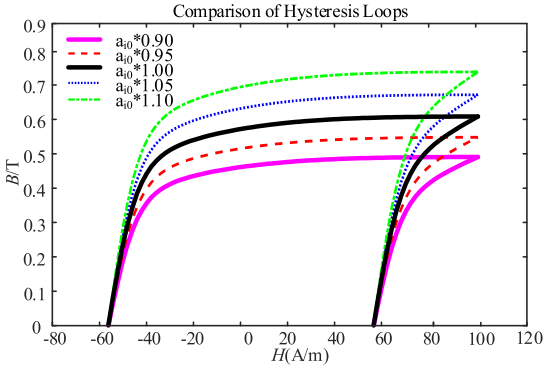

FIGURE 3. Hysteresis loops under different a_i.

The hysteresis loops corresponding to different a_i values are shown in Figure 3. Figure 3 shows that B_p, B_r and S_{hb} are affected by the change in a_i, and their trends are positively correlated with that of a_i; the change in a_i has almost no effect on the H_c of the hysteresis loop.

TABLE 2. Variation of shape parameters under different a_i.

a_i	B_p/T	H_c (A/m)	B_r/T	S_{hb} (T•A/m)	K_{pr}	K_{cr} (A/m/T)
$0.90a_{i0}$	0.509	56.269	0.480	111.463	1.060	117.204
$0.95a_{i0}$	0.567	56.269	0.535	124.192	1.060	105.196
$1.0a_{i0}$	0.629	56.269	0.593	137.609	1.060	94.937
$1.05a_{i0}$	0.693	56.269	0.654	151.713	1.060	85.999
$1.10a_{i0}$	0.761	56.269	0.717	166.506	1.061	78.468

As shown in Table 2, as a_i increases, B_p, B_r, and S_{hb} all increase by the same proportions, K_{cr} reduces in equal proportions, while H_c and K_{pr} remain almost unchanged. When a_i increases by 5%, B_p, B_r, and S_{hb} increase by about 10.5%; K_{cr} decreases by about 10%; K_{pr} increases by about 0.08%; and H_c remains unchanged. According to the variation data of the hysteresis loop index,it can be seen that for the same variation of a_i, the variation of B_p, B_r, K_{cr} and S_{hb} is significantly higher than that of other indicators.

C. EFFECT OF PARAMETER b_i VARIATION ON HYSTERESIS LOOP SHAPE

The variation rules of b_i are the same as those of a_i. Change the value of parameter b_i in Table 1, multiply the value of $b_1 \sim b_3$ as the reference value by the same time at the same multiplier to realize the increase or decrease of the value of b_i, and keep the value of a_i, b_i and c_i in Table 1 unchanged. Take the values of $b_1 \sim b_3$ in Table 1 as the base value b_{i0} and multiply them by 0.90, 0.95, 1.05, 1.10 times respectively to get four groups of b_i parameter values, and substituting the four groups of different parameter values into the APM shown in (8). The graphs of the hysteresis loops corresponding to the different b_i parameter values are obtained by programming as shown in Figure 4, and the values of H_c, B_r, B_p, K_{cr}, S_{hb} and K_{pr} are listed in Table 3.

The different lines in Figure 4 represent the hysteresis loops at different values of b_i. Figure 4 shows that the variation of b_i has some effect on the H_c, B_r, B_p, K_{cr}, S_{hb} and K_{pr}, but the variation trends are different. H_c, K_{cr} and S_{hb} are positively correlated with those of the trends of b_i, while the trends of B_r, B_p, and K_{pr} are opposite to them.

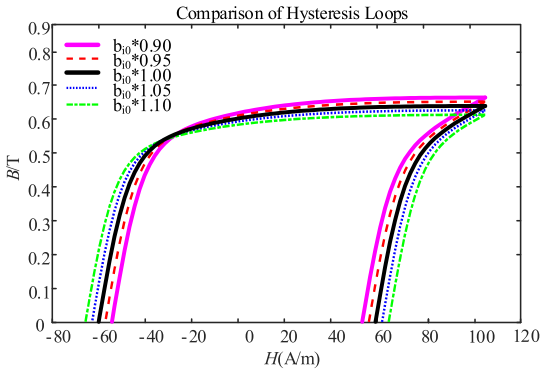

FIGURE 4. Hysteresis loops under different b_i.

TABLE 3. Variation of shape parameters under different b_i.

b_i	B_p/T	H_c (A/m)	B_r/T	S_{hb} (T•A/m)	K_{pr}	K_{cr} (A/m/T)
$0.90b_{i0}$	0.653	50.131	0.609	130.511	1.073	82.344
$0.95b_{i0}$	0.641	54.223	0.601	134.173	1.067	90.207
$1.0b_{i0}$	0.629	56.269	0.593	137.609	1.060	94.937
$1.05b_{i0}$	0.616	58.316	0.584	140.841	1.055	99.907
$1.10b_{i0}$	0.603	62.408	0.575	143.886	1.049	108.611

As shown in Table 3, as b_i increases, H_c, K_{cr} and S_{hb} increase, and B_p, B_r, and K_{pr} decrease. As b_i increases by 5%, H_c increases by about 5.5%, K_{cr} increases by about 5.0∼9.5%, S_{hb} increases by about 2.4%, B_p decreases by about 2.1%, B_r decreases by about 1.5%, and K_{pr} decreases by about 0.5%. Based on the results of the quantitative analysis above, it can be concluded that for the same variation in b_i, the variation of K_{cr} and H_c is higher than that of other indicators.

D. EFFECT OF PARAMETER c_i VARIATION ON HYSTERESIS LOOP SHAPE

The variation rules of c_i are also the same as those of a_i. Change the value of parameter c_i in Table 1, multiply the value of $c_1 \sim c_3$ as the base value by the same multiplier at the same time to realize the increase or decrease of the value of c_i, and leave the value of a_i, b_i and b_i in Table 1 unchanged. Taking the values of $c_1 \sim c_3$ in Table 1 as the base value c_{i0} and multiplying them by 0.90, 0.95, 1.05, 1.10 times respectively to obtain four groups of c_i. The four sets of different parameter values are substituted into APM in (8). The hysteresis loops corresponding to the different c_i parameter values are obtained by programming as shown in Figure 5, and the values of the coercivity H_c, remanent magnetization point B_r, saturation magnetic induction strength B_p, loop area S_{hb}, slope factor K_{cr} and rectangular ratio K_{pr} are given in Table 4.

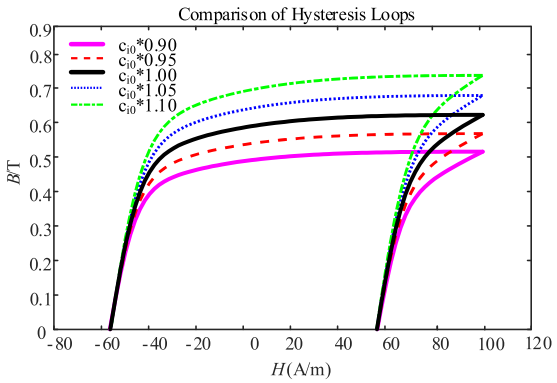

FIGURE 5. Hysteresis loops under different c_i.

The different lines in Figure 5 represent the hysteresis loops at different values of c_i. From Figure 4, it can be seen that the variation of c_i. has some effect on the B_p, B_r, K_{pr}, K_{cr} and S_{hb}, while it has almost no effect on H_c. c_i has significant positive correlations with B_p, B_r, and S_{hb}, negative correlations with K_{cr}, and positive correlations with K_{pr}.

TABLE 4. Variation of shape parameters under different c_i.

c_i	B_p/T	H_c (A/m)	B_r/T	S_{hb} (T•A/m)	K_{pr}	K_{cr} (A/m/T)
$0.90c_{i0}$	0.520	56.269	0.493	115.083	1.055	114.067
$0.95c_{i0}$	0.573	56.269	0.542	126.129	1.058	103.799
$1.0c_{i0}$	0.629	56.269	0.593	137.609	1.060	94.937
$1.05c_{i0}$	0.686	56.269	0.645	149.514	1.063	87.212
$1.10c_{i0}$	0.745	56.269	0.610	161.837	1.065	80.442

As shown in Table 4, when c_i for every 5% increase, the increase in B_p, B_r, S_{hb} and K_{pr} is approximately 9.2%, 9.0%, 8.8%, and 0.2%, respectively. K_{cr} decreases by about $7 \sim 9\%$. H_c remains essentially unchanged. According to the analysis of the data in Table 4, under the same variation in c_i, the changes in B_p, B_r, K_{cr} and S_{hb} are similar and higher than those in K_{pr} and H_c.

E. EFFECT OF IRREVERSIBLE MAGNETIZATION PARAMETERS ON HYSTERESIS LOOP SHAPE

Changing the irreversible magnetization parameters of the APM affects the coercivity H_c, remanent magnetization point B_r, magnetic induction intensity at the vertex of loop B_p, loop area S_{hb}, slope factor K_{cr} and rectangular ratio K_{pr}. According to the computational and analytical results presented in Figures 3-5 and Tables 2-4, the variation rules and trends of the hysteresis loops are calculated and obtained as shown in Table 5, when the irreversible magnetization parameters a_i, b_i and c_i are varied respectively. In Table 5, "↑" indicates increasing, "–" indicates no or little change, and "↓" indicates decreasing.

TABLE 5. Variation law of hysteresis loop shape when model parameters change.

	B_p/T	H_c (A/m)	B_r/T	S_{hb} (T•A/m)	K_{pr}	K_{cr} (A/m/T)
$a_i\uparrow$	↑	–	↑	↑	–	↓
$b_i\uparrow$	↓	↑	↓	↑	↓	↑
$c_i\uparrow$	↑	–	↑	↑	↑	↓

From Figures 2-4 and Tables 2-5, the parameter a_i mainly affects B_p, B_r S_{hb} and K_{cr}, and with the growth of a_i, the B_p, B_r and S_{hb} grow with the same rate, K_{cr} decreases; the parameter b_i affects H_c, B_p, B_r, S_{hb}, K_{cr} and K_{pr}, where H_c has the greatest variation and K_{pr} has the smallest variation; with the increase of b_i, H_c, K_{cr}, and S_{hb} increase, and B_p, B_r, S_{hb} and K_{pr} decrease; the parameter c_i has a more significant effect on K_{cr} and K_{pr} compared with the parameter b_i. As c_i increases, B_p, B_r, S_{hb} and K_{pr} increases, K_{cr} decreases.

In particular, when the parameters a_i, b_i, and c_i are changed in the decreasing direction, the trend of the hysteresis loop shape characteristic parameters is opposite to that shown in Table 5.

IV. APPLICATION OF LAW OF HYSTERESIS LOOP SHAPE CHANGING WITH PARAMETERS

The APM shown in (8) has 12 parameters. Due to the large number of model parameters, it is very difficult to accurately determine the parameter values. The preliminary parameter values obtained through parameter identification often cannot meet the accuracy requirements of the hysteresis loop calculation. For example, in Figure 6(a), there is a significant deviation between the simulated hysteresis loop (red line) and the measured hysteresis loop (black line), indicating that the model parameter values are not accurate enough. In this case, based on the influence of the previous parameter changes on the shape of the hysteresis loop, the corresponding parameter values can be continuously adjusted according to the characteristics of the deviation between the

simulated loop and the measured loop. Finally, the required parameter values can be obtained, so that the simulated loop matches the measured loop.

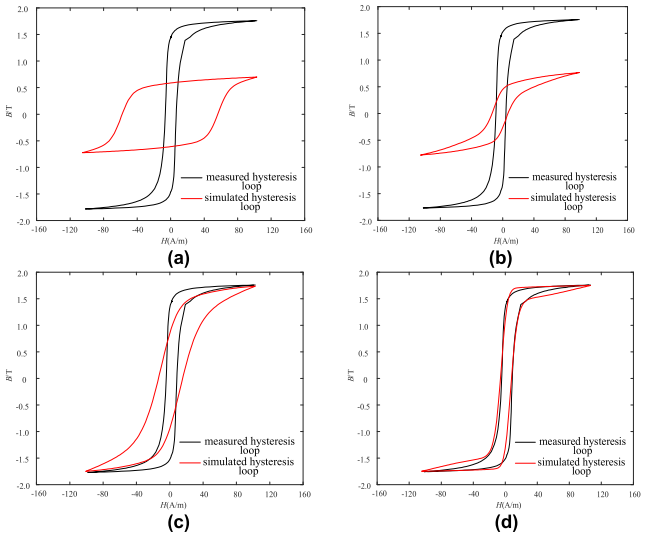

FIGURE 6. Adjust model parameters based on the impact of parameter changes.

The simulated loop in Figure 6(a) has a higher coercivity than the measured one. According to the law in Table 5, the first step is to reduce b_i to achieve a reduction in coercivity until it approaches the coercivity of the measured loop. Finally, the red loop in Figure 6(b) is obtained.

The magnetic flux density at the turning point of the simulated loop in Figure 6(b) is lower than that measured. According to the influence law in Table 5, the second step is to increase a_i and c_i to increase the magnetic flux density at the turning point of the loop until it approaches the magnetic flux density of the measured loop. Finally, the red loop in Figure 6(c) is obtained.

The coercivity, inclination, and rectangular ratio of the simulated loop in Figure 6(c) are all greater than those measured. According to the influence law in Table 5, the third step can be to first reduce b_i and then increase a_i or c_i. By continuously adjusting the parameter values, the simulated loop in Figure 6(d) can be obtained which matches the measured loop.

The above application cases, based on the influence of parameters on the hysteresis loop, adjust the parameter values to achieve consistency between the simulated loop and the measured loop, demonstrating the applicability of the law obtained in this study.

V. CONCLUSION

In this paper, the variation of the irreversible magnetization parameters a_i, b_i, and c_i of the APM on the coercivity H_c, remanence point B_r, magnetic induction intensity at the loop vertex B_p, loop area S_{hb}, slope factor K_{cr} and rectangular ratio K_{pr} of the hysteresis loop are investigated by the one-factor-variable method, and the trends and laws of the hysteresis loop shape a_i, b_i, and c_i are summarized based on the analysis of the data of the effects of the parameter variations on the hysteresis loop shape.

The variation of parameter a_i affects only B_p, B_r S_{hb} and K_{cr}, and has no effects on H_c and K_{pr}. When the parameter a_i changes, B_p, B_r and S_{hb} change in the same proportion.

The variation of parameter b_i affects H_c, B_p, B_r, S_{hb}, K_{cr} and K_{pr}, with the greatest effect on H_c. The parameter b_i is the determining factor H_c.

The variation of parameter c_i effects B_p, B_r, S_{hb}, K_{pr} and K_{cr}, and has no effects on H_c. The parameter c_i has a more obvious influence on K_{pr} than the parameter b_i, and the parameter c_i is the main influencing factor of K_{pr}.

REFERENCES

[1] I. D. Mayergoyz, "Mathematical models of hysteresis," *Phys. Rev. Lett.*, vol. 56, no. 15, pp. 1518–1524, Apr. 1986.

[2] Z. G. Zhao, P. Zhang, and X. W. Ma, "Magnetic characteristic simulation of electrical steel sheet based on improved Preisach model," (in Chinese), *High Volt. Eng.*, vol. 47, no. 6, pp. 2149–2157, Sep. 2021.

[3] X. Zhao, X. Liu, and L. Li, "Hysteretic and loss modeling of silicon steel sheet under the DC biased magnetization based on the Preisach model," in *Proc. 22nd Int. Conf. Electr. Mach. Syst. (ICEMS)*, Harbin, China, Aug. 2019, pp. 1–6, doi: 10.1109/ICEMS.2019.8921745.

[4] S. Hussain and D. A. Lowther, "An efficient implementation of the classical Preisach model," *IEEE Trans. Magn.*, vol. 54, no. 3, pp. 1–4, Mar. 2018, doi: 10.1109/TMAG.2017.2748100.

[5] S. E. Zirka, Y. I. Moroz, P. Marketos, and A. J. Moses, "Congruency-based hysteresis models for transient simulation," *IEEE Trans. Magn.*, vol. 40, no. 2, pp. 390–399, Mar. 2004, doi: 10.1109/TMAG.2004.824137.

[6] G. Bertotti, *Hysteresis in Magnetism: For Physicists, Materials Scientists, and Engineers*. San Diego, CA, USA: Academic, Apr. 1998.

[7] V. De Santis, A. Di Francesco, and A. G. D'Aloia, "A numerical comparison between Preisach, J–A and D-D-D hysteresis models in computational electromagnetics," *Appl. Sci.*, vol. 13, no. 8, p. 5181, Apr. 2023, doi: 10.3390/app13085181.

[8] Z. Szabó and J. Füzi, "Implementation and identification of Preisach type hysteresis models with Everett function in closed form," *J. Magn. Magn. Mater.*, vol. 406, pp. 251–258, May 2016, doi: 10.1016/j.jmmm.2016.01.027.

[9] R. Liu, Y. X. Du, and L. Li, "Derivation and modification of analytical positive Preisach hysteresis model," (in Chinese), *Proc. CSEE*, vol. 43, no. 5, pp. 2070–2079, Apr. 2023, doi: 10.13334/j.0258-8013.pcsee.212979.

[10] Y. L. Li, L. Li, and R. Liu, "Comparative analysis and evaluation of static characteristics of two simplified Preisach models," *Adv. Technol. Electri. Eng. Energy*, vol. 39, no. 5, pp. 25–31, Jun. 2020.

[11] L. Spinu, I. D. Borcia, A. Stancu, and C. J. O'Connor, "Time and temperature-dependent Preisach models," *Phys. B, Condens. Matter*, vol. 306, nos. 1–4, pp. 166–171, Dec. 2001, doi: 10.1016/S0921-4526(01)00998-X.

[12] B. Chen, Q. L. Zeng, and F. R. Wang, "Error correction and characteristic parameter identification method of analytical Preisach hysteresis model under variable temperature conditions," *Adv. Technol. Electri. Eng. Energy*, vol. 43, no. 6, pp. 60–69, Jun. 2024.

[13] B. Chen, F. Wang, N. Wan, B. Tang, and L. Huang, "Analytical Preisach hysteresis model considering reversible component and its characteristic parameter identification algorithm," (in Chinese), *High Voltage. Eng.*, vol. 49, no. 11, pp. 4766–4774, Nov. 2023, doi: 10.13336/j.1003-6520.hve.20220260.

[14] L. Chen, L. Cui, T. Ben, and L. Jing, "An improved Preisach distribution function identification method considering the reversible magnetization," *CES Trans. Electr. Mach. Syst.*, vol. 7, no. 4, pp. 351–357, Dec. 2023, doi: 10.30941/CESTEMS.2023.00038.

[15] D. D. Li, B. K. Jie, and S. L. Zhu, "Parameter identification of analytical Preisach model based on improved chimpanzee algorithm," *Sci. Technol. Eng.*, vol. 24, no. 17, pp. 7140–7147, Sep. 2024, doi: 10.12404/j.issn.1671-1815.2304783.

[16] B. Guang-qing and H. Lei, "Parameter identification and verification of Preisach hysteresis model based on cosh function," *J. Magn. Mater. Devices*, vol. 51, no. 2, pp. 24–29, Mar. 2020, doi: 10.19594/j.cnki.09.19701.2020.02.006.
[17] Y. L. Li, L. Li, and R. Liu, "Identification of distribution function for static inverse Preisach model based on non-uniform element discretization method," *Proc. CSEE*, vol. 41, no. 15, pp. 5340–5351, Sep. 2021, doi: 10.13334/j.0258-8013.pcsee.200363.
[18] L. Zhu, Z. Sun, X. Wei, and H. Dai, "An improved discrete Preisach model of open circuit voltage hysteresis for $LiFePO_4$ batteries," in *Proc. IEEE Vehicle Power Propuls. Conf. (VPPC)*, Montreal, QC, Canada, Oct. 2015, pp. 1–8, doi: 10.1109/VPPC.2015.7352895.
[19] D. Jiles, *Introduction to Magnetism and Magnetic Materials*, 3rd ed., Boca Raton, FL, USA: CRC Press, 2015.
[20] L. H. Lewis, A. Mubarok, E. Poirier, N. Bordeaux, P. Manchanda, A. Kashyap, R. Skomski, J. Goldstein, F. E. Pinkerton, R. K. Mishra, R. C. Kubic Jr., and K. Barmak, "Inspired by nature: Investigating tetrataenite for permanent magnet applications," *J. Phys., Condens. Matter*, vol. 26, no. 6, Feb. 2014, Art. no. 064213, doi: 10.1088/0953-8984/26/6/064213.
[21] R. Liu, Y. X. Du, and L. Li, "Analytical inverse Preisach hysteresis model," *Trans. China Electrotech. Soc.*, vol. 38, no. 10, pp. 2567–2576, Sep. 2023, doi: 10.19595/j.cnki.1000-6753.tces.220467.

HUIYING ZHANG was born in Shangqiu, Henan, China, in 1980. She received the bachelor's degree in electrical engineering and the master's degree in control theory and control from Henan Polytechnic University, in 2003 and 2008, respectively, and the Ph.D. degree in electrical engineering from Lanzhou Jiaotong University, in 2021. She has been a Teacher with the School of Automation and Electrical Engineering, Lanzhou Jiaotong University, since 2021. Her main research interests include electromagnetic equipment modeling and simulation, magnetization characteristic modeling, reactive power compensation equipment modeling and control, and power quality analysis.

YADONG SHEN was born in Wuwei, Gansu, China, in 1999. He received the bachelor's degree in electrical engineering from Lanzhou Jiaotong University, in 2022, where he is currently pursuing the master's degree in electrical engineering.

MINGXING TIAN was born in Gansu, China, in 1968. He is currently a Professor with the School of Automation and Electrical Engineering, Lanzhou Jiaotong University. His main research interests include analysis and control of power quality in power systems, design and control of electrical machine and electric appliance, and power electronics technology and its application.